Architecture
Image Studies

Vol.7, Issue 1, pp.354-377, 2026
DOI: https://doi.org/10.62754/ais.v7i1.848

https://journals.ap2.pt/index.php/ais/index

Enhanced Cluster Head Selection Based Resource Allocation with Hybrid PSO and Modified Moth Flame Optimization in Cognitive Radio Networks for IoT Applications

T. Vijaya Kumar[1], Madona B Sahaai[2], C. Sharanya[3]

Abstract

The enhanced cluster head selection-based resource allocation with hybrid PSO and modified moth flame optimization in cognitive radio networks for IoT applications (ECHRAC) approach proposed by IBM aims to reduce power consumption and increase energy efficiency in Cognitive Radio Network (CRN) nodes through an advanced method, which is highly sophisticated. ECHRAC employs a dual-phase approach that efficiently selects the cluster head (CH) and uses specialized algorithms in conjunction with inverse optimization methods. Spectrum sensing plays a crucial role in the selection of CH. Using primary user (PU) channels by clusters of secondary users will enhance spectrum access and decrease interference during this phase. ECHRAC employs a delicate approach to the probabilistic framework that manages false alarms, setting up high detection thresholds in such synchronization to prevent interference with PU. The ECHRAC's cluster formation and path selection phase is given significant attention. Nodes in the CRN are dynamically clustered according to the availability of the spectrum and their proximity to nodes. A complex selection procedure is involved in this stage, which identifies nodes with optimal energy and connectivity attributes for CH roles. ECHRAC employs a unique energy state function that utilizes Energy Harvesting (EH) to determine the cluster's CH status. This encompasses energy harvested, battery status, and energy consumption for data forwarding and control signaling. By selecting CHs through a competitive process, nodes that meet these energy requirements are selected to maintain varying amounts of energy across the network. ECHRAC employs an energy-based control system that divides nodes into active, sleep and dead states based on their remaining energy to improve the reliability of data transmission. This mechanism minimizes energy depletion risk, which permits nodes in low-power states to prioritize crucial tasks or switch to sleep mode to conserve energy. A hybrid approach is employed during the optimization phase, which involves combining an Improved Particle Swarm Optimization (PSO) algorithm with the Modified Moth Flame Optimization (MFO) Algorithm. ECHRAC's PSO algorithm utilizes a particle-based representation scheme to represent potential solutions, while also considering the optimization of node parameters for efficient clustering and route selection. By using a logarithmic spiral function, the MFO algorithm dynamically alters the paths of CH nodes to achieve optimal convergence towards high-fitness node convection, while minimizing the need for flames in each iteration. By utilizing dual optimization techniques, network longevity, and throughput are improved, and data transmission reliability is enhanced by prioritizing routes with energy-efficient CH nodes. Simulation results show that ECHRAC has a significant impact on several performance metrics of CRN. This model is implemented using MATLAB software, focusing on parameters such as network throughput, power usage, energy efficiency, data delivery ratio, and average delay for performance analysis.

Keywords: *Cognitive radio network (CRN), cluster head (CH), primary user (PU), Energy Harvesting (EH), Modified Moth Flame Optimization (MFO), Particle Swarm Optimization (PSO), Enhanced CH Selection, Resource Allocation, and Hybrid Optimization Process.*

[1] Research Scholar, Vels Institute of Science, Technology & Advanced Studies, Chennai, TN, India
[2] Assistant Professor, Vels Institute of Science, Technology & Advanced Studies, Chennai, TN, India..
[3] Assistant Professor, Sathyabama Institute of Science and Technology, Chennai, TN, India

Introduction

The concept of the Internet of Things (IoT) entails a network where digital devices communicate autonomously, without requiring human or computer intervention. This concept has become widespread in our daily lives. To accommodate the increasing use of IoT, CRNs were incorporated, creating the Cognitive Radio Internet of Things (CRIoT). This integration provides the necessary spectrum for IoT to continue to grow and advance. The term IoT has gained significant attention lately [1]. Various technologies and studies have been utilized to facilitate the widespread growth of IoT. The expected influence of IoT on our everyday lives and habits is significant. Essentially, IoT encompasses a worldwide network of connected objects, often called "things," such as computing devices, mechanical tools, and machinery. These objects are interconnected and provided with IP addresses to facilitate communication across networks. While both wired and wireless connections are possible, wireless connections are preferred due to their flexibility [2]. IoT aims to allow these objects to communicate without human intervention. IoT devices typically have low cost, power consumption, battery life, data transfer rate, coverage range, storage capacity, processing capabilities, and limited scope. On the other hand, IoT networks have a large number of connections and utilize simple protocols.

Cognitive Radio (CR) is an intelligent and flexible communication tool that interacts with its environment to collect data on its radio frequency surroundings, internal conditions, location, and application requirements. This enables the radio to dynamically modify its operational settings—such as transmission power, frequency, communication protocols, and modulation—in real-time to accomplish its intended communication objectives. Due to the rapid expansion of the Internet of Things (IoT), there has been a notable rise in the volume of data that must be transmitted across the spectrum band. [3]. However, due to its limited availability, spectrum scarcity is a major concern. This scarcity is not only dependent on channel availability but also on spectrum utilization and the technologies being used. The traditional approach of assigning fixed spectrums is no longer sufficient and purchasing additional spectrums can be costly. For IoT to continue growing as expected, IoT technology must integrate with CR capabilities. This will allow IoT devices to access unused licensed spectrums, improving spectrum efficiency by providing opportunistic access for IoT devices [4].

Using CRN for the implementation of the IoT intelligent network is a cost-effective and effective approach to address the issue of limited spectrum in the IoT. The merging of CR technology with the IoT, known as CRIoT, is poised to offer diverse applications, especially in time-critical sectors like intelligent healthcare and transportation.[5]. The integration of these technologies necessitates meeting a spectrum of network needs, such as channel availability, allocation, end-to-end latency, dependability, energy efficiency, and enhanced data transfer rates. To address the escalating connectivity demands from numerous IoT applications utilizing CR technology, a diverse range of communication standards and technologies becomes essential. In indoor smart environments, options like Bluetooth, ZigBee, and Wi-Fi are employed, whereas outdoor scenarios necessitate the use of cellular systems such as IEEE 802.11af and Weightless. By harnessing the capabilities of CRN, both short and long-distance communications can be effectively supported. [6].

The key responsibilities of IoT smart networks involve the detection of channels free from interference amidst PU activity, assessing the effectiveness of these detected opportunities, ensuring seamless communication as IoT devices switch channels due to the presence or movement of PUs, and overseeing access to licensed spectrum for a multitude of IoT devices while minimizing any disruption to PUs. [7]. Additionally, Figure 1 depicts the key design elements of a CRIoT system, including the intended application and its specific features, the technology employed for device communication and its unique attributes, and any regulations imposed by the country in which it is utilized, such as licensing requirements, acceptable levels of interference, and certification protocols [8].

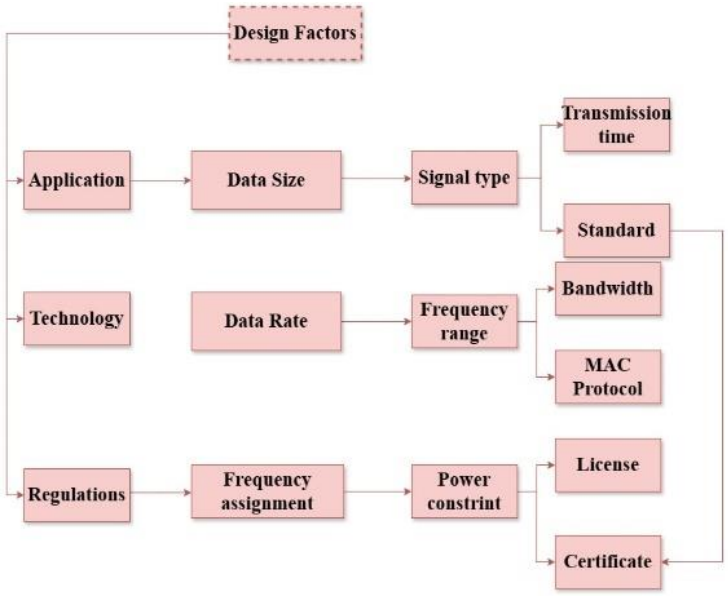

Figure 1 - CRIoT system

Clustering is a commonly used method for managing a large number of nodes in a network. In CR networks, cognitive users have the option to form groups based on geographical or operational factors. Within these groups, a cognitive user is chosen as the CH. The CH collects sensing information from all secondary users in the group and reports it to the Fusion Center on their behalf. If the CH is far from the Fusion center, they will share this information with the nearest CH at regular intervals to reduce energy consumption during reporting. After each cooperative sensing process, a final decision is reported to the Fusion Center, improving energy efficiency in CR networks [9]. The majority of optimization issues are not convex and this makes it challenging to discover a worldwide optimal resolution because they have multiple solutions. When dealing with optimization problems that have a vast search space or are more intricate, traditional mathematical algorithms may struggle to find a solution. However, various metaheuristic optimization algorithms available in research have proven to be highly effective in solving complex optimization problems. Each of these algorithms has its unique advantages and room for enhancement. While some may converge quickly, others may require more time to find the optimal solution [10]. The process of effective CH selection and proper resource allocation among the CRNs-based IoT applications are still in open research. To overcome such drawbacks this article enhanced CH selection-based resource allocation with hybrid optimization. The major contribution of this article is described below.

Research Contribution:

- To improve the efficiency of the CR-IoT environment, an enhanced CH selection process is initiated and the devices are properly communicated with required resource allocation.
- Followed by that, the hybrid optimization is carried out with the presence of the PSO algorithm and Modified MFO algorithm which helps to increase the communication efficiency of the devices in the CR-IoT environment.
- The experimental demonstration includes the CR-IoT network construction and several scenarios with performance metrics. The parameters which are specified for the hybrid optimization and cluster modules are analyzed.

Related Works

In [11], unmanned aerial vehicles (UAVs) are used as relays in a collaborative Cognitive Internet of Things (CIoT) system, with energy-harvesting power sources being integrated into the DF relay strategy. In [12], the Jaya algorithm optimizes processes efficiently by navigating the search space, achieving impressive computational performance in power allocation. In [13], tree-centric spectrum allocation in CRNs is a method to reduce underutilization, where a centralized base station manages channel distribution in real-time to SUs based on availability. In [14], current methods average 10-12 attempts with a 315 ms delay, new approach averages 1-2 attempts with a 72 ms delay. In [15], pa-Jaya is a new approach for power allocation in cognitive OFDM radio networks for IoT, utilizing swarm

intelligence principles. In [16], the Jaya algorithm performs well regardless of spectrum types, offering improved convergence rates and transmission performance in simulations. In [17], the PA-Jaya algorithm optimizes processes by efficiently searching the space to solve power allocation problems with high performance. In [18], the protocol aims to resolve hidden primary terminal problems, maintain priority rights for PUs, and optimize spectrum sensing periods to maximize system performance. In [19], PUs retain priority rights to the spectrum, even in densely deployed CR networks. This prioritization is crucial for ensuring that critical communications are not disrupted by secondary users' activities. In [20], a new system architecture for multi-band CR-enabled SG communication aims to optimize sensing time and power allocation. In [21], optimization techniques maximize data rate and ensure minimum detection probabilities for active PUs. Simulation validates methods. In [22], the HTSA algorithm combines tabu search and simulation to achieve Pareto optimality between EE and SE, supported by a fuzzy decision-making system. Simulation results show its effectiveness in various resource allocation scenarios. In [23], a VOS viewer layout algorithms aid data visualization. Cognitive radio use, spectrum sensing, and opportunist spectrum access improve efficiency. In [24], a fuzzy-based approach with a look-up table was used to improve energy and spectrum efficiency in 5G networks. Simulations in NS-2.31 and MATLAB visualization showed enhanced system performance. In [25], performance metrics such as achievable throughput, average cluster count, and energy consumption are evaluated for the proposed CBCSS method and contrasted with optimal algorithms. In [26], the clustering protocol for CRWSN incorporates evolutionary game theory, enhancing network stability and scalability. It outperforms current methods with a 25% increase in selecting high-energy CHs and promotes a more even geographical distribution by 37%. Additionally, it reduces energy consumption by 23% and extends the network's lifetime by 27%. In [27], a four-phase communication protocol was created to enhance time allocation for maximizing SCP in an energy-limited MEC network in IIoT. Two algorithms, SCPM-GSS and SCPM-GA, optimized EH time for CHs, improving SCP by 3% to 30% compared to fixed parameters, particularly at lower to medium power levels. Monte Carlo simulations validated these enhancements. In [28], a new channel assignment method for SUs in CRNs uses a tree structure and centralized base station. It reduces channel acquisition attempts to 1-2 with a delay of 72 ms, surpassing previous methods needing 4-10 attempts with delays of 128-315 ms.

System Fundamentals:

The system fundamentals of the CRN network consist of innovative network architecture, details about the required system parameters, and utilities, and they are described in Figure 2.

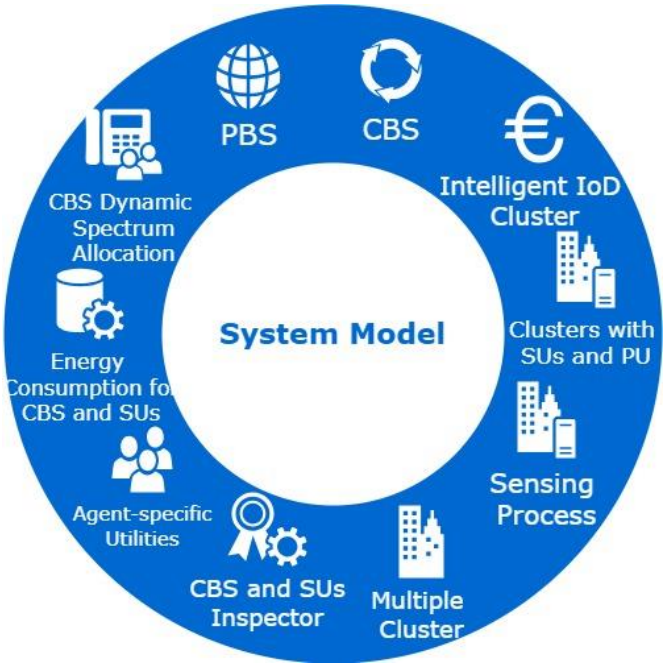

Figure 2 – System Model

Network Architecture

Intelligent IoD (SU) clusters are distributed across the CRN, as seen in Figure 3**.** It is described as follows: PBS is the Primary Base Station, and CBS is the Cognitive Base Station. The clusters are

under CBS authority. Every cluster keeps an eye on a PU, and when the PU is absent, the SUs in each cluster work together to acquire its frequency band cooperatively. Every subunit estimates the channel before beginning the spectrum access procedure. Each super unit chooses the optimal spectrum allocation based on the channel circumstances. If there are more than one PU, SUs will create several clusters continuously with every cluster representing a separate PU. The actions carried out in a single cluster are specifically the subject of this work; the other clusters will use the same method. Centralized CRNs have a problem in that individual cluster members may not perceive PU activity collaboratively; instead, they may rely on other cluster members to transmit their sensing data to the CBS. Because of this, we must continually verify if SUs is picking up spectrum signals. A subclass of game theory known as inspection games may be used to describe this circumstance. Two sides are often involved in inspection games. SUs, or inspectors, are the first group that must perceive the spectrum. But to conserve energy, SUs often remain undetected. To verify if SUs is indeed sensing the spectrum, the CBS acts as the monitoring party.

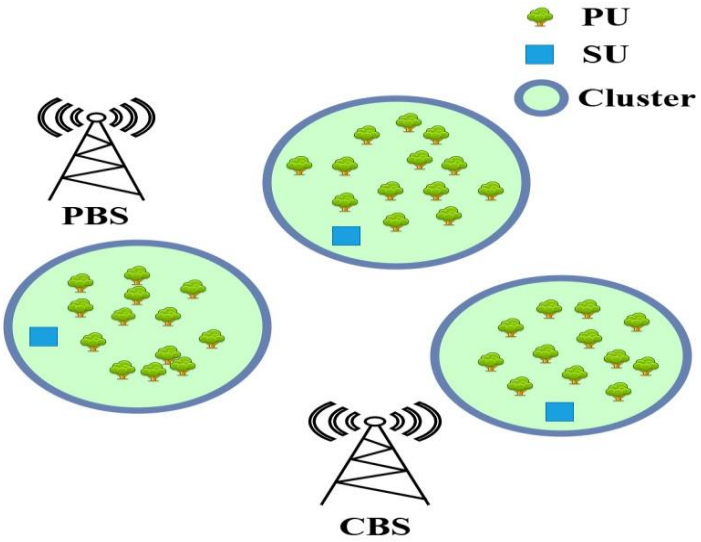

Figure 3 - Intelligent CRN Structure

Network parameters

Since 'n' represents the count of SUs within the cluster, we define a set 'N' that includes these SUs: N = {1, 2, ..., n}. Thus, all individuals' respective technique sets and the set of every single agent can be expressed by

$$A = N \cup \{CBS\} \tag{1}$$

$$S_i = \{\sigma_i : \sigma_i \epsilon Z^+, \sigma_i^{min} \leq \sigma_i \leq \sigma_i^{max}, i \epsilon N\} \tag{2}$$

$$S_{CBS} = \{\eta : \eta \epsilon Z^+, \eta^{min} \leq \eta^{max}, \sigma_i^{min} \leq \eta^{min} \; and \; \sigma_i^{max} \leq \eta^{max} \forall i\} \tag{3}$$

Here, 'S' denotes the set of possible strategies, 'σi' represents the sensing rates, and 'η' signifies the inspection rates. 'A' encompasses the finite group of all agents involved, including both SUs and the CBS entity. Consider that the Appendix has a thorough description of every notation. Sensing frequencies σ_i serve as the basis for SUs' tactics S_i, as they possess the ability to perceive or not. Alternatively, the CBS has the option to conduct an inspection or not. As a result, the approach suggested by SCBS is mostly dependent on the examination rate η. Because both sides' approaches indicate the total amount of sensing and examinations per period, as demonstrated in equations (2) to (3), the strategies for the SUs and the CBS are defined as positive whole numbers. Understanding the relationship between the bounds of each party's strategy$\sigma_i^{min} \leq \eta^{min} \; and \; \sigma_i^{max} \leq \eta^{max}$ as well as how they affect the network is also essential. The 3 potential outcomes in the CRN that can arise if the agents choose the maximum techniques from the strategy groups are depicted in Figure 4**.** To keep things simple, we concentrate on only one SU i and the CBS. The CBS did not inspect the first situation ($\sigma_i^{max} \leq \eta^{max}$), where the SU skipped the subsequent time unit's detection of the spectrum procedure. For this reason, in situation A, the CBS is inept. At all times during scenarios B and C, the CBS consistently observes the actions of the SUs. Thus, maximizing $\sigma_i^{max} \leq \eta^{max}$ and minimizing

similarity$\sigma_i^{min} \leq \eta^{min}$ is the ideal course of action. SUs are more likely to be caught in either of these scenarios.

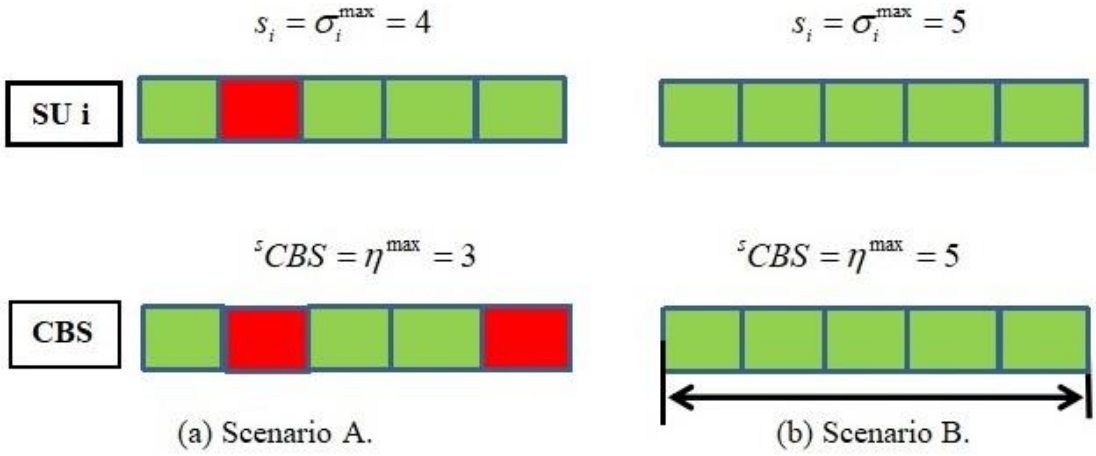

Figure 4 – Strategic Details

Utility Function

The utility function, which might be stated as follows, is how we describe the communications between entities in this system.

$$U_a(X, S_a) = (B_a(x) - w \times C_a S_a), \text{ where } S_a \in S_a \text{ and } a \in A \quad (4)$$

$$C_a(S_a) = \frac{S_a}{\max\{S_a\}} \quad (5)$$

Here, 'w' represents the relative weight, 'C' denotes the cost function, 'U' signifies the utility function, 'B' stands for the benefit function, and 's' represents the selected strategy from the set of strategies 'S'. It should be noted that for clarity, the terms within the utility function have been standardized. The quantity of energy that the agent received in exchange for the approach it selected, denoted by the abstract term C_a. The benefit function B_a is interpreted differently by each participant than the cost function.

$$B_i(x) = \frac{x_i - \left[\frac{1}{n-1}\left(\sum p_i^j \times \max\{x_j - x_i, 0\}\right)\right]}{x_i^{max}} \quad \text{Where i, j } \epsilon \text{ N and i≠j} \quad (6)$$

$$p_i^j = \frac{\left(\frac{x_j}{x_j^{max} - x_j^{max}}\right)}{\left(\frac{x_i}{x_i^{max} - x_i^{max}}\right)} \quad \text{Where i, j } \epsilon \text{ N and i≠j} \quad (7)$$

Here, 'p' represents the psychological factor, 'n' denotes the count of SUs within the cluster, and 'x' signifies the desired amount of spectrum. The SU benefit function B_i characterizes the needed spectrum as it appears in Equation (6). It is calculated as follows: the preferred quantity of spectrum x_i is subtracted from the median psychological loss. It is the SU itself that causes the typical psychological loss. When the desired amount of spectrum by a Secondary User (SU) is lower than that of other SUs within the same cluster, it experiences a psychological disadvantage when compared. If the desired quantity is more than the requested amount, there won't be any psychological harm. When comparing SU's desired quantity to SU's, the psychological component p_i^j indicates the weight assigned to SU's psychological loss. For efficient spectrum sharing, the CBS is responsible not only for observing the actions of SUs but also for dynamically allocating the available spectrum bands to them. Concerning the distribution of spectrum for SUs, the ASR is represented by the benefit function of CBS.

Proposed ECHRAC Approach

This proposed ECHRAC approach is mainly developed to reduce power utilization and increase the efficiency of the CRN network nodes. The core modules of this process are the efficient CH selection process and hybrid optimization model which is described in Figure 5.

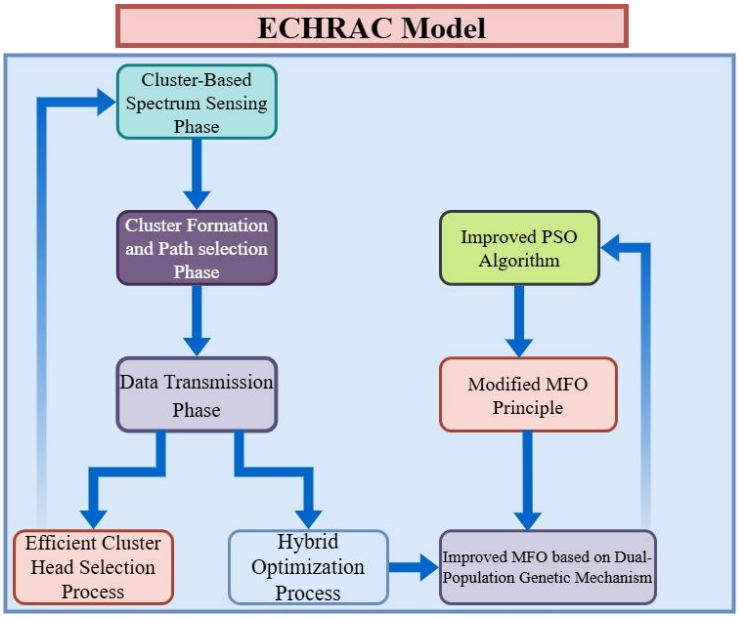

Figure 5 – Architectural Diagram of Proposed ECHRAC

Efficient CH Selection Process

Cluster-Based Spectrum Sensing Phase:

Assume a CRN with M PU channels and N SUs. The PU is the only entity using any given channel. However, the PU is inactive, and the SU may use spectrum sensing to take advantage of the channel when it becomes accessible. Let N be the set of SUs and M be the set for these PU channels. The channel heterogeneity-spectrum accessibility differs amongst the SUs. Only in situations where the PUs' detection capability only includes a portion of the overall system would the distant SUs report noise. The CRN is therefore divided into clusters such that each cluster's SUs are inside the identical set of PU channels' identification range. Figure 6 illustrates the spectrum sensing model which is utilized for the clustering process.

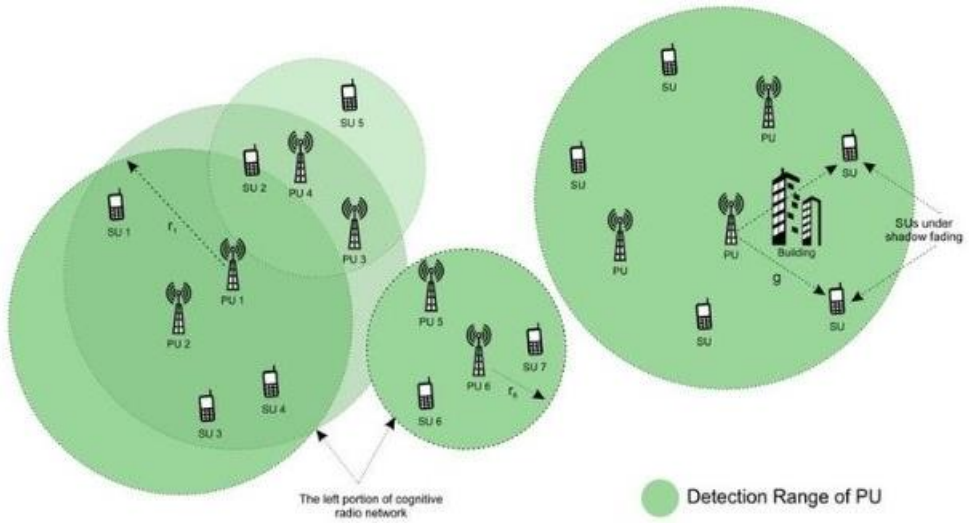

Figure 6 - Spectrum Sensing Model

Only CR users can assign the unoccupied piece of the spectrum. The frequency is sampled using a sampling frequency, f_s.

$$H_j^1 : y_{i,j}(k) = s_{i,j}(k) + u_{i,j}(k)\ i = 1, 2, \ldots, N \quad (8)$$

$$H_j^0 : y_{i,j}(k) = u_{i,j}(k)\ i = 1, 2, \ldots, N \quad (9)$$

The probabilistic value of the $s_{i,j}$ withinH_j^0, that is provided by, is the definition of the false alarm probabilities $P_{f,(i,j)}$

$$P_{f,(i,j)} = Q\left(\left(\frac{\epsilon_i}{\sigma^2_{u_{i,j}}} - 1\right)\sqrt{f_s T}\right) \tag{10}$$

$P_{d,(i,j)}$ is the definition of the detection probability which is represented as follows

$$P_{d,(i,j)} = Q\left(\left(\frac{\epsilon_i}{\sigma^2_{u_{i,j}}} - 1 - \gamma_{i,j}\right)\sqrt{\frac{f_s T}{2\gamma_{i,j}+1}}\right) \tag{11}$$

Maintaining the detection probability over a certain value Q_{th}, that is, $P_{d,(i,j)}) \geq Q_{th}$ is necessary to ensure that each Pus receives sufficient defence. Therefore,

$$\prod_{i=1}^{m}(1 - P_{d,(i,j)}) \geq Q_{th} \tag{12}$$

The allocation matrices for the PU and Sus are $[X_s]_{NXK}$ and $[X_c]_{MXK}$. The following defines the elements $x_{s,i}^k$ and $x_{c,j}^k$:

$$x_{s,i}^k \begin{cases} 1 \; if \; SU \; is \; with \; cluster \\ r \\ 0 \; otherwise \end{cases} \tag{13}$$

$$x_{c,j}^k \begin{cases} 1 \; if \; CH_j \; is \; with \; cluster \\ r \\ 0 \; otherwise \end{cases} \tag{14}$$

Observe the next two vectors that are provided, for cluster k, S_k stood for the set of SUs.

$$S_k = \left\{ i | x_{s,i}^k = 1, \forall i \; \epsilon \; N \; \right\} \tag{15}$$

Cluster's SUs sense and use a set of PU channels, which is indicated by B_k.

$$B_k = \left\{ j | x_{c,j}^k = 1, \forall i \; \epsilon \; M \; \right\} \tag{16}$$

Consequently, the overall throughput is determined by

$$R_k(S_k, B_k) = \sum_{j£\mathrm{Bk}} \frac{T-\tau}{T} \; P \; (H_j) C_j (1 - Q_{f,j}^k \; (S_k, B_k)) \tag{17}$$

In the case of channel j, $P(H_j)$ represents the idle probability, C_j denotes the transfer capacity, and

$$Q_{f,j}^k \; (S_k, B_k) = 1 - \prod_{i \epsilon S_k} \left(1 - P_{f,(i,j)} \left(\frac{\tau}{b_k}\right)\right) \tag{18}$$

A 3D matrix called A_{NXMXK} is defined to reflect the assignment policy.

$$A_{ijk}^n \begin{cases} 1 \; if \; i \; \epsilon \; S_k \; and \; \epsilon \; B_k \\ - \\ 0 \; otherwise \end{cases} \tag{19}$$

After formulation, the issue is stated as

$$max_{X_s, X_c,} = \sum_k R_k(\, S_k(X_s), B_k(X_c)) \tag{20}$$

$$\sum_{k=1}^{K} x_{s,i}^k = 1, \forall i \tag{21}$$

$$\sum_{k=1}^{K} x_{c,j}^k = 1, \forall \; j \tag{22}$$

$$\sum_{i \epsilon S_k} x_{s,i}^k \geq \overline{m}, \forall k \tag{23}$$

Only when the associated choice problem is resolved can the optimization challenge be handled in polynomial time. Accordingly, demonstrating a method for an optimization issue is the same as proving the choice issue that goes along with it.

Cluster Formation and Path Selection Phase

The proposed cluster formation and route setup stage consists of three main sub-stages: first, the selection of CHs, followed by the construction of clusters, and finally, the selection of routes.

CHs selection sub-stage: In the process of selecting CHs, the first ring of surviving nodes within the CRN is immediately designated as CHs. For the other surviving nodes in subsequent rings, node 'j' calculates the total number of neighbors within the same ring and cluster radius '$num(j)$' through exchanged control information. Additionally, 'Next(j)' represents the count of neighboring nodes in the outer ring that share the most available channels within the maximum communication range 'Rt'. Node 'j' then computes the total energy used for processing data from neighboring residents within the same ring and cluster radius, denoted as 'E forward(j)', along with the energy needed for data forwarding to outer rings, and the energy utilized for control data exchange, as described by Equations (24) – (26). These computations, as shown in Equation (27), contribute to the determination of the EH-based energy state function. This function takes into account the node's remaining energy and the energy it has harvested.

$$E_{control}(j) = 3L_1 \times (E_{elec} + E_{fs} \times R_{r(j)}^2) + 3L_1 \times (N_{r(j)} - 1) \quad (24)$$

$$E_{intra}(j) = \left(N_{r(j)} - 1\right) \times E_{elec} \times L_2 + N_{r(j)} \times E_{DA} \times L_2 + ((E_{elec} + E_{fs} \times d_{CH(j)\to router(r(j)-1)}^2) \times L_2 \quad (25)$$

$$E_{forward}(j) = \frac{\sum_{k=r(j)+1}^{z} \frac{A_k}{S_k}}{\frac{A_{r(j)}}{S_{r(j)}}} \times \left[E_{elec} + E_{fs} \times d_{CH(j)\to router(r(j)-1)}^2\right] \times L_2 \quad (26)$$

$$EH\_ESF(j) = \begin{cases} E_{res}(j) + E_{EH}(j) - E_{control}(j) - E_{forward}(j) & if\ r(j) = 1 \\ E_{res}(j) + E_{EH}(j) - E_{control}(j) - E_{intra}(j) - E_{forward}(j) & otherwise \end{cases} \quad (27)$$

Where the dimensions of the information and control packets are represented by the variables L_1 and L_2, correspondingly; The electrical circuitry's consumption of energy for sending and receiving just one bit of data is represented by E_{elec}; The energy needed to gather one unit of data is denoted by EDA; the average number of nodes in a single cluster of rings $r(j)$ is represented by, and the energy consumption per bit by the power amplifier is indicated by. The symbol signifies the total volume of data packets required to be transmitted from outer rings by ring $r(j)$, while denotes the area of the ring $r(j)$. Additionally, represents the average area of a single cluster in a ring $r(j)$. Lastly, signifies the average distance between the CHs in the ring $r(j)$ and either the sink or the relay CHs in the ring $r(j) - 1$. Equation (28) illustrates how node 'j' calculates the EH-based CHs selection weight $EH\_W(j)\ using\ EH\_ESF(j)$.

$$EH_{W(j)} = \begin{cases} [\alpha \times EH\_ESF(j)]^2 \times \sqrt[3]{c(j)} \times \sqrt{\frac{1}{d_{tosink(j)}}} \times \frac{1}{Next_{(j)}} \times \sqrt[3]{num(j)} & if r(j) \neq 1 \cap Next(j) \neq 0 \\ 0 & if\ Next\ (j) = 0 \\ \alpha \times EH\_[ESF(j)]^2 \times \sqrt[3]{c(j)} \times \sqrt{\frac{1}{d_{tosink(j)}}} \times \frac{1}{Next_{(j)}} & if r(j) = 1 \cap Next(j) \neq 0 \end{cases} \quad (28)$$

The energy state function's effect is adjusted by α, which is a weight factor. Nodes having non-zero remaining energy beyond the primary ring transmit their CHs weights inside the cluster radius after the CHs being chosen weight $EH_{W(j)}$ is established. These nodes compare the CH weights after receiving these weights from their neighbours. When a node's total weight drops below that of one of its neighbors, it broadcasts a message on CCC announcing its decision to withdraw from the competition, which is received by nearby nodes. On the contrary, when a node possesses the highest weight among all its neighboring nodes, it becomes a CH and sends out a CH declaration message on the CCC, prompting nearby nodes to respond in kind. This process continues until every node has either exited the competition or become a CH.

Cluster sub-stage of construction: Ordinary nodes that have not yet joined a cluster identify the CH with the highest weight and the most shared available channels within their transmission range., they submit a join request to that CH, indicating that they have formed a cluster. Following their listing as respective CMs, CHs accept these join requests coming from regular nodes. When regular nodes

can't find a CH, they automatically take on the role of a CH. Clusters are formed autonomously by CHs that don't get any join requests. After each ordinary node has determined which CH it belongs to, cluster creation is finished, and the procedure proceeds to the route selection sub-stage.

Route sub-stage of selection: To be more precise, nodes in the first ring can transmit packets straight to the sink since they can get there in just one hop. All CHs that are located within the first ring must choose suitable relay nodes to help forward data packets so they can arrive near the sink since there are communication distance limits. In the final upper ring, the CH 'j' selects a pair of inner-ring CHs, denoted as 'a' and 'b', that maximize the competition score $'Compet(j)'$ and store this information. If an insufficient number of suitable nodes are found, CH 'j' seeks assistance from its Cluster Member (CM) 'k' to identify the next hops. Eventually, it identifies two relay nodes, 'a' and 'b', that enhance $'Compet(j)'$. CH 'j' then chooses the next-hop relay in the following ring from the inner-ring CH 'a' that enhances $'Compet(j)'$. The route selection process concludes when CH 'j' records two-hop relays, 'k' and 'a', that optimize $'Compet(j)'$ if they are available. If only a few such relays are found, CH 'j' utilizes its CM 'k' to search for the next hop. Equation (10) presents the formula for the competition score $'Compet(j)'$.

$$Compet\ (j) = \begin{cases} EH\_W(a) & if\ r(j) = 2, CM\ k \notin relay \\ EH\_W(a)\ \times EH\_W(k) & if\ r(j) = 2, CM\ k \in relay \\ EH\_W(a)\ \times EH\_W(b) & if\ r(j) \geq 3, CM\ k \notin relay \\ EH\_W(a)\ \times EH\_W(b) \times EH\_W(k) & if\ r(j) \geq 3, CM\ k \in relay \end{cases} \quad (29)$$

Where relay refers to the group of relays made up of CMs.

Data Transmission Phase

Nodes go to the data transmission phase following the conclusion of the cluster creation and route construction phases. CRSN nodes will nevertheless significantly deplete their energy due to frequent data transfer and relay. To prevent CRSN nodes from excessive contention during data transmission, an energy status control system has been incorporated into the proposed protocol locations from dying too soon from a lack of energy, which could result in the transmission of data errors, and hinder wasteful use of energy from overbearing stimulation of the SWIPT process.

Through this process, a Sj of CRSN node j state is separated into three distinct categories based on its remaining energy $E_{res}(j)$: active state $Sactive$, sleep state S_{sleep}, and dead state S_{death}. $E_{res}(j)$ below Edeath means that the node is in the dead state (S_{death}), with no energy left to execute any tasks and no ability to keep tabs on the surroundings. The node assumes the state of sleep S_{sleep}, utilizing simply linear EH and refraining from data transfer, relay, or similar activities, to safeguard against vitality depletion when $E_{res(j)}$ is equal or greater than to E_{death} yet lower than its dormancy threshold $E_{dormancy}(j)$. In the active state S_{active}, the node can perform energy-intensive activities, provided it has enough remaining energy left over after $E_{dormancy}(j) < E_{res}(j) \leq E_{max}$. The energy used in the control information interchange, intra-cluster data receiving, aggregation, and forwarding, and the help relaying data from outside layers every round, make up the dormancy threshold $E_{dormancy}(j)$ for CH(j), as Equation (30) illustrates.

$$E_{dormancy}(j) = 3L_1 \times \left(E_{elec} + E_{fs} \times R_{r(j)}^2\right) + 3L_1 \times E_{elec} \times \left(N_{r(j)} - 1\right) + \left(N_{r(j)} - 1\right) \times E_{elec} \times L_2 + N_{r(j)} \times E_{DA} \times L_2 + L_2 \times \left(E_{elec} + E_{fs} \times d_{CH(j)\rightarrow router(r(j)+1)}^2\right) + \frac{\sum_{k=r(j)+1}^{z} N_{CH}(k) \times (2E_{elec} + E_{fs} \times d_{CH(j)\rightarrow router(r(j)+1)}^2) \times L_2}{N_{CH}(r(j))} \quad (30)$$

Where, $d_{CH(j)\rightarrow router(r(j)+1)}$ represents The Euclidean distance between CH 'j' and its next-hop relay is represented by 'd'; 'n(j)' quantifies the number of CHs in the same ring as CH 'j'; and 'P' $\sum_{k=r(j)+1}^{z} N_{CH}(k) / N_{CH}(r(j))$ denotes the number of data packets CH 'j' assists in relaying. The dormancy threshold 'D' $E_{dormancy}\ (k)$ for CM 'k' is the energy required for data transmission to the CH and the exchange of control information in each round.

$$E_{dormancy}(k) = 3L_1 \times \left(E_{elec} + E_{fs} \times R_{r(j)}^2\right) + 2L_1 \times E_{elec} \times \left(N_{r(j)} - 1\right) + 2L_1 \times E_{elec} + L_2 \times (E_{elec} + E_{fs} \times d_{CM(k)\rightarrow CH}^2 \quad (31)$$

The distance between CM 'k' and its CH is indicated by 'd', while 'r' represents the cluster radius of the layer where CM 'k' is located by $R_{r(k)}$.algorithm 1 describes the efficient CH selection process for CRSN in detail.

Algorithm 1 – Efficient CH Selection Process for CRSN

Input: CRN parameters are M for the PU channel, N for SU, Q_{th} for threshold detection probability, f_s for sampling frequency, T for the sensing period, E_{elec} for energy per bit for transmission, E_{fs} for free-space model energy, E_{DA} for energy for data aggregation, L_1, L_2 for control and data packet sizes, Rt for maximum communication range, α for weight factor for CH selection, and distance between nodes of rings.

Output: CH selection, assigned SU to each CH, route selection for each relay for each CH to the sink, and data transmission control.

Cluster-based spectrum sensing phase for $SU\ i\ and\ PU\ j$

The compute channel is occupied $H_j^1: y_{i,j}(k) = s_{i,j}(k) + u_{i,j}(k)\ i = 1, 2, \ldots, N, and$ channel is free $H_j^0: y_{i,j}(k) = u_{i,j}(k)\ i = 1, 2, \ldots, N$.

Calculate false alarm probability $P_{f,(,j)}$ and detection probability $P_{d,(i,j)}$ using $P_{f,(i,j)} = Q\left(\left(\frac{\epsilon_i}{\sigma^2_{u_{i,j}}} - 1\right)\sqrt{f_s T}\right)$ and $P_{d,(i,j)} = Q\left(\left(\frac{\epsilon_i}{\sigma^2_{u_{i,j}}} - 1 - \gamma_{i,j}\right)\sqrt{\frac{f_s T}{2\gamma_{i,j}+1}}\right)$, and ensure $P_{d,(i,j)} \geq Q_{th}$ provide PU protection.

CH selection phase remaining energy $E_{res}(j)$ for SU, Rt, cluster radius.

For each energy state function $EH\_ESF(j)$:

$$EH_{ESF(j)} = E_{res}(j) + E_{EH}(j) - E_{control}(j) - E_{intra}(j) - E_{forward}(j)$$

Calculate CH weight $EH_{W(j)}$:

$$EH_{w(j)} = \alpha.[EH_{ESF(j)}]^2.\sqrt{\frac{1}{d}\,to\ sink(j)}$$

Broadcast CH weights within the cluster radius and the height weight becomes CH and broadcast CH declaration.

The cluster formation phase identifies the CH with the highest weight within the transmission range and requests the CH to form a cluster no CH is found, the node becomes a CH.

Path selection phase, for $CH\ j$ in the upper ring, identify two inner – rings CH a and b that maximize the competition score $Compet(j)$.

End for

SU states based on energy levels for

State $S_{active,}, S_{sleep}, S_{dead}\ based\ on\ remaing\ energy\ E_{res}(j)$, and transmit data in an active state, switch to sleep or dead state.

End for

Hybrid Optimization Process

Improved PSO Algorithm

Observing the flock of birds serves as the inspiration for PSO, a bio-inspired optimization approach. All the solutions in PSO are called "particles," and each one is like a bird in the swarm. A swarm comprising S particles is initialized at the start of the cycle. To represent a particle, let $x_i^k = [x_{i1}^k, x_{i2}^k, \ldots, x_{iD}^k]$ represent its location at iteration k for particle *i* (1≤*i* ≤*S*), where D is the number of dimensions. Binary numbers from {0,1} are accepted by x_{id}^k . $y_i^k = [y_{i1}^k, y_{i2}^k, \ldots, y_{iD}^k], y_{id}^k \in R$ is the notation for the interaction k is the velocity of a particle. Fitness values, which represent each particle's suitability for an optimization goal, are assigned to each swarm member.

The formulas $p_i^k = [p_{i1}^k, p_{i2}^k, \ldots, p_{iD}^k]$ and $p_g^k = [p_{g1}^k, p_{g2}^k, \ldots, p_{gD}^k]$ are used to represent the optimal solution reached by the entire swarm up are iteration k and particle i, respectively. Every time there is an iteration, every particle modifies its velocity based on its previous velocity, the distance to its best solution, and the distance to the swarm's best solution. Following is an update on the particle's velocity:

$$y_{id}^{k} = y_{id}^{k-1} + \xi_2 r_2 (p_{gd}^{k-1} - x_{id}^{k-1}) \quad (32)$$

The range [0,1] values random values are equal to r_1 and r_2, and ξ_1 and ξ_2 constitute two significant constants. In addition, the sigmoid function that follows is used to convert the velocity to a number in the interval [0,1]:

$$sig\left(y_{id}^{k}\right) = \frac{1}{1+\exp(-y_{id}^{k})} \quad (33)$$

Where is the probability of x_{id}^{k} taking 1 is indicated by s $sig\left(y_{id}^{k}\right)$. $sig\left(y_{id}^{k}\right)$ indicates that x_{id}^{k} might be modified as,

$$x_{id}^{k} = \begin{cases} 1, & if\ r < sig\left(y_{id}^{k}\right) \\ 0, & else \end{cases} \quad (34)$$

In [0,1], r is a uniformly distributed random number. $sig\left(y_{id}^{k}\right)$ approaching 0 or 1 is prevented in a maximum velocity V_{max} is using the distance PSO. To utilize PSO for problem-solving, each particle is mapped to a potential solution. The particle's position consists of binary bits, while the visiting order is represented by decimal values. Therefore, we must convert the binary bits to decimal numbers or the other way around. Following startup, every particle's fitness is assessed. In order to get fitness function, we employ the reverse of the handoff delay. A new particle swarm is produced after the fitness evaluation is complete, with (32) and (34) updating the velocity and location.

Modified MFO Basic Principle

Using the principles of moth behavior in their quest for light, MFO is an efficient optimization technique. The moth population is represented by M, which may be described as

$$M = \begin{bmatrix} M_{11} & M_{12} & \dots & M_{1d} \\ M_{21} & M_{22} & \dots & M_{2d} \\ \vdots & \vdots & \vdots & \vdots \\ M_{n1} & M_{n2} & \dots & M_{nd} \end{bmatrix} \quad (35)$$

In this case, d denotes the solution's dimension and n the population size. Suppose that OM is the moth population's fitness value vector. It is possible to get,

$$OM = \begin{bmatrix} OM_1 \\ OM_2 \\ \vdots \\ OM_n \end{bmatrix} \quad (36)$$

Assign F to the flame set. It is possible to get

$$F = \begin{bmatrix} F_{11} & F_{12} & \dots & F_{1d} \\ F_{21} & F_{22} & \dots & F_{2d} \\ \vdots & \vdots & \vdots & \vdots \\ F_{n1} & F_{n2} & \dots & F_{nd} \end{bmatrix} \quad (37)$$

Assume that OF is the flame set's fitness value vector, which is written as

$$OM = \begin{bmatrix} OF_1 \\ OF_2 \\ \vdots \\ OF_n \end{bmatrix} \quad (38)$$

A triple abstraction can be used to represent the MFO optimization process.

MFO = (I, P, T) (39)

In this instance, I am the randomly produced flame sets and moth populations' initialization behavior. Next is the computation of its fitness value, whose value is as follows:

$$\mathrm{I}: \phi \rightarrow \{M, OM\} \quad (40)$$

According to the logarithmic spiral function, T is the moth's unique updated behavior. The moth individual uses the logarithmic spiral function to update themselves depending on the flame set and its present condition. It might be stated as

$$\begin{cases} M_i = S(M_i, F_i) = D_{ij} e^{\tau l} \cos(2\pi l) + F_j \\ D_{ij} = |M_i i - F_j| \end{cases} \quad (41)$$

Where logarithmic spiral morphological constant τ is, here, $'l'$ is a random number ranging from -1 to 1, $S(M_i, F_i)$ represents the logarithmic spiral function, where M_i stands for the ith individual moth, 'Fj' represents the jth flame, and D_{ij} signifies the straight-line distance between the ith individual moth and the jth flame. P is the way moth populations behave as they update their trajectories in Equation (42). Updates to the moth's fitness value will be made if they are greater than those of the flame. This may be stated as

P: M, F → F (42)

In each repetition, the quantity of flames will steadily decrease. The following formula is used to specifically update the number of flames.

$$n_f = round\ (n - t\frac{n-1}{t_{max}}) \quad (43)$$

In this case, round(x) denotes rounding x to the closest integer, t is present iterations numbers, and t_{max} is the greatest number of repetitions.

Enhanced MFO with Dual-Population Genetic Mechanism

In contrast to conventional optimum technology, MFO's strong algorithm convergence, straightforward parameterization, and computational structure have drawn the interest of several academics. Additionally, its practical use in the field of optimization issues has grown. But as the calculations go, a significant portion of the moth species will rapidly approach a specific flame location if it offers clear benefits. Premature convergence of the method is likely to occur if the local optimum already has a location in flame, as this is going to render it difficult for the moth population to find an alternative. With the aid of a dual populace, this study incorporates the dual-population genetic process in an attempt to address the problem of the MFO's easy descent into localized convergence. The objective is to improve the global optimization capability of the MFO by efficiently guiding each moth towards the current optimal flame during the iterative process, the MFO helps to accelerate convergence and global optimization while offering orientation assistance for the genetic moth–flame population's evolution. Meanwhile, even after the moth population reaches a local extremum, it will continue to hunt for optimization because of a dual genetic process. Algorithm 2, discussed the performance of hybrid PSO-MFO.

A certain amount of evolutionary disruption is brought about in the moth population's evolution procedure through operators of crossover, selection, and mutation are the three. This helps the population avoid the problem of local convergence and improves its entire optimization efficiency. Global optimization performance is too high for conventional genetics to match with dual populations. It is challenging for the method to achieve global convergence during the lengthy iteration stage of the conventional genetic procedure because the ideal person has some "domination" throughout the population. Subsequently, the perfect member of the basic communities readily maintains the long-established "dominant" position due to changes in the population environment. In the dual population system, the most appropriate individuals from two populations can engage in exchange activities.

Algorithm 2 – Hybrid PSO-MFO

Input: objective function $f(x)$, population size S, number of iterations t_{max}, dimension D, initial position and velocities, and a cognitive and social coefficient for PSO.

Output: best solution x_{best}, and best fitness value $f(x_{best})$.

Randomly initialize the position x_i^0 and velocities y_i^0 for each particle i in PSO, and moth position M and flames F for MFO.

The best position for each particle p_i^0 and initialize the global best position p_g^0, and initialize dual-population if enabled.

For $k = 1\ to\ t_{max}/2$

For particle i:

Calculate fitness $f(x_i^k)$,

Update p_i^k if $f(x_i^k)$ is better than the previous p_i^{k-1}, global best p_g^k if $f(p_i^k)$ is better than $f(p_g^{k-1})$, velocity y_i^k using $y_i^k = y_i^{k-1} + \xi_1 r_1\left(p_i^{k-1} - x_i^{k-1}\right) + \xi_2 r_2\left(p_g^{k-1} - x_i^{k-1}\right)$

Sigmoid function to map velocity to Probability $sig\left(y_{id}^k\right) = \frac{1}{1+\exp(-y_{id}^k)}$, and position $x_{id}^k = \begin{cases} 1, & if\ r < sig\left(y_{id}^k\right) \\ 0, & else \end{cases}$.

End for

End for

MFO phase with a dual population in iteration $t - t_{max}/2$+1 to t_{max};

Calculate the number of flames n_f using, $n_f = round(S - t.\frac{S-1}{t_{max}})$

For the position based on flame F_j using the logarithmic spiral function $M_i = D_{ij}.e^{\tau.l}.\cos(2\pi.l) + F_j$.

Calculate fitness OM_i for each moth M_i, if $f(M_i) < f(F_j)$, flame position F_j.

End for

Weight coefficient adaptive strategy coefficient ω using: $\omega = \omega_{min} + (\omega_{max} - \omega_{min}).\cos\left(\left(\left(1 - \frac{t}{t_{max}}\right).\frac{\pi}{2}\right)^{\beta}\right.$ and adjust F_j position using the ω for improved convergence control.

Return completing t_{max} iterations, the best solution x_{best} and fitness $f(x_{best})$.

Weight Coefficient Adaptive Nonlinear Decreasing Strategy for

One important metric for MFO is the weight coefficient. Details of the weight coefficient moth position update equation are shown below.

$$\begin{cases} M_i = S(M_i, F_i) = D_{ij}e^{\tau l}\cos(2\pi l) + wF_j \\ D_{ij} = |M_i i - F_j| \end{cases} \quad (44)$$

The inertia weight is represented by ω. To make the algorithm's search range narrower and therefore increase the optimization capability of the entire optimization procedure, a good technique for reducing the weight coefficient ought to be suggested. An adaptive nonlinear decreasing approach for the weight coefficient is necessary due to the nonlinear nature of the entire MFO optimization process, ensuring a closer representation of the real-world scenario. An approach to weight coefficient ω with strong flexibility that is nonlinear and relies on cosine form lowering is presented in this study. This is the weight coefficient $\omega's$ calculation formula.

$$\omega = \omega_{min} + \omega_d.\cos\left((1 - t_r).\frac{\pi}{2}\right)^{\beta} \quad (45)$$

In this case, ω_d represents the weight coefficient's decreasing amount, $\omega_{max} - \omega_{min}$ represents the weight coefficient's highest and minimum values, respectively; Iteration progress is represented by $t_r = t \cdot t_{max} - 1$, and the optimization factor is denoted by β.

It can be observed that the weight coefficient is falling nonlinearly, and this trend will persist throughout the repetitive computation procedure as the evolution generation changes. The nonlinear decline method in Figure 7 illustrates how choosing the best optimization factor β allows the cosine to achieve maximum efficiency and modify the nonlinear decline trend. A high capacity to adapt and be flexible characterizes this approach. In order to enhance the algorithm's capacity for global optimization, this technique may modify the weight coefficient's drop rate in immediate terms throughout the process of iteration. This helps to better balance the effects of neighborhood growth and worldwide exploration. Moreover, this study preserves a level of global exploration capability by implementing a gradual decrease in speed, which is proportional to the weight coefficient, during the final stage [0.8, 1] of the optimization process.

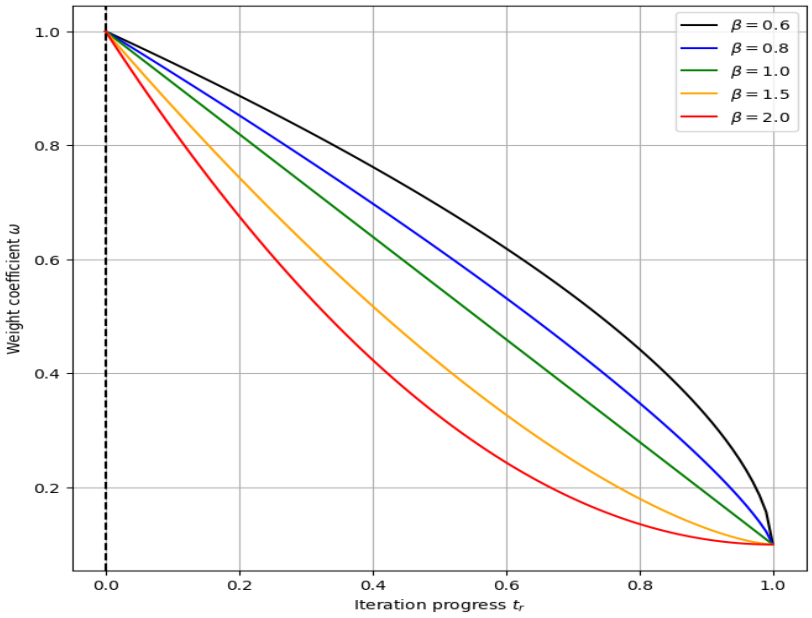

Figure 7 - The evolutionary algebra and weight coefficient connection

Performance Analyses

The simulation demonstration of the proposed ECHRAC approach is implemented in the MATLAB software. It is, also known as Matrix Laboratory, an advanced coding language and interactive platform primarily created for numerical calculations, data examination, and graphical representation. Created by MathWorks, MATLAB offers a wide range of features and capabilities for diverse fields of science and engineering. The performance evaluation of the proposed ECHRAC approach is conducted and compared with previous methods such as GTNCC [26], OMIEH [27], and ICACI [28]. The input parameters that are used for this simulation are given in Table 1.

Table 1 – Simulation Input Parameters

Parameters	Values
Node deployment area	200*200
No. of. sensor nodes	200
No. of. primary users	4
No. of. secondary users	13
Initial energy	0.5J
Transmission power	500mw
Transmission range	20m
Max velocity	20m/s
Time limit	60s

Performance of the ECHRAC Approach

Convergence Plot: In the field of hybrid optimization and CH selection in CRN networks, convergence refers to the gradual approach of an algorithm toward a solution, as the values of the objective function or fitness metric become stable or reach a consistent level. Figure 8 visually illustrates how the performance of the hybrid PSO and MFO optimization changes with each iteration. Here, the x-axis denotes the number of iterations, whereas the y-axis indicates the best cost value achieved. The convergence plot is useful in monitoring the progress of the proposed ECHRAC over time, evaluating its speed in reaching an optimal solution, and determining if it is stuck in a local minimum or still exploring different solutions. This information can then be used to determine when to stop the proposed optimization process.

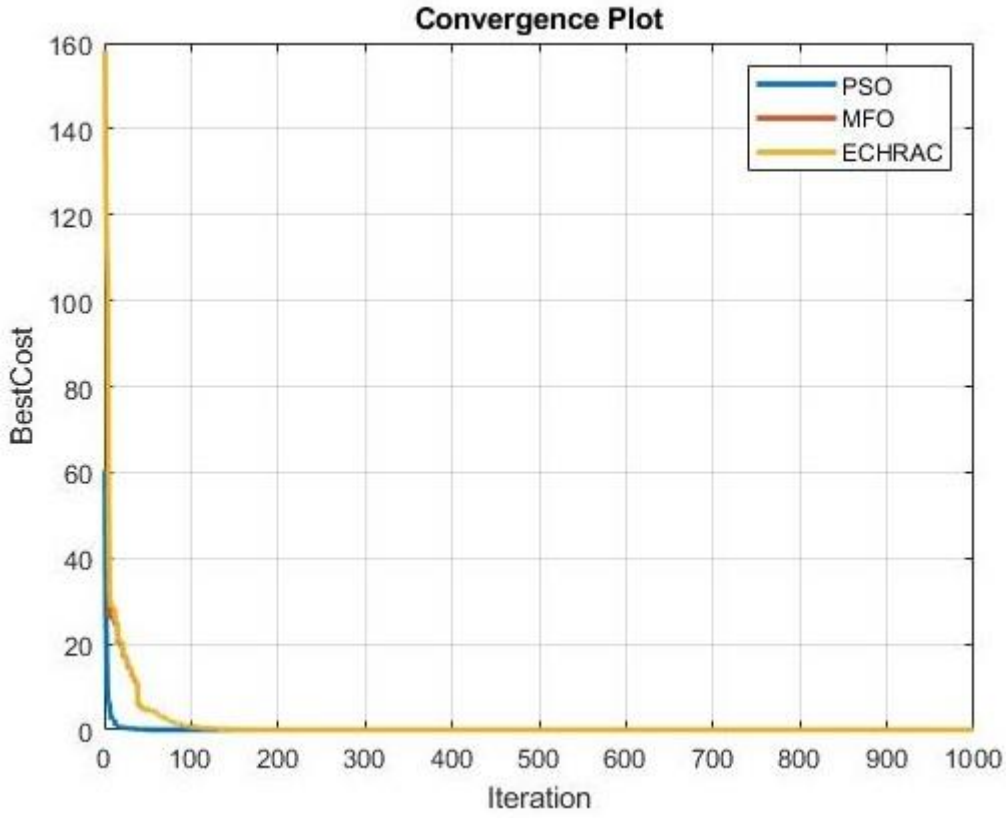

Figure 8 – Convergence Plot

Total Error Rate Vs Threshold Value: The error rate is determined by the extent to which the achieved solution differs from the desired one, thanks to the integration of hybrid optimization and efficient cluster processing. This measure can be tailored to specific objectives, constraints, or performance criteria that are relevant to the problem at hand in the CRN network model. Figure 9 provides a visual representation of how the hybrid PSO and MFO optimization perform in terms of total error rate. The threshold value denotes the x-axis, while the total error rate of ECHRAC represents the y-axis. This metric offers a comprehensive evaluation of the optimization process, taking into account communication efficiency, resource utilization, and overall system objectives. It can effectively gauge how well the hybrid optimization model is progressing toward an optimal or near-optimal solution for CH selection and resource allocation.

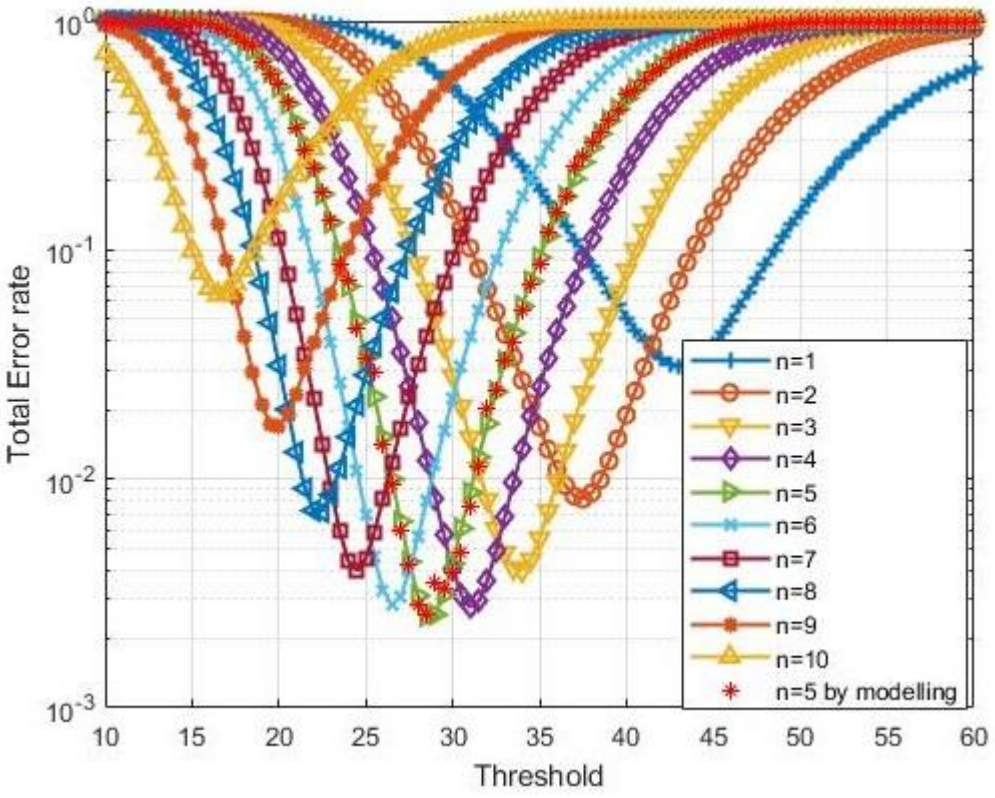

Figure 9 – Total Error Rate

Cluster Assignments and Centroids Measures: The CRN network model with hybrid optimization utilizes cluster assignments to group CRN nodes according to specific criteria. These assignments are crucial in CH selection-based resource allocation as they determine which nodes are chosen as CHs and which belong to each cluster. These assignments also play a role in determining the communication structure of the network. In the context of CH selection, a centroid serves as a representative point that summarizes the characteristics of a cluster, typically calculated as the mean of feature values from all data points within the cluster. A visual representation in Figure 10 illustrates the performance of hybrid PSO and MFO optimization in terms of cluster assignments and centroids measures.

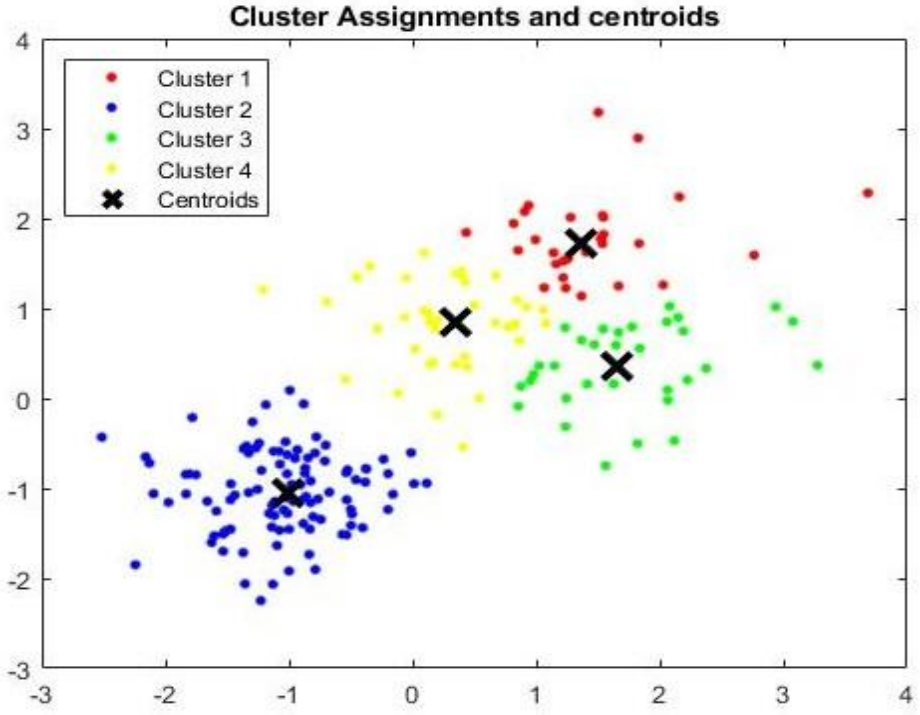

Figure 10 – Cluster Assignments and Centroids

Comparative Analysis

Total Energy Consumption: In the context of CH selection-based resource allocation and a hybrid optimization model, Total Energy Consumption refers to the combined energy used by CRN nodes during communication. This is an important metric for evaluating the energy efficiency of both the CH selection process and the overall network. It allows for an assessment of how effectively the hybrid optimization model, incorporating PSO and MFO, is managing and allocating energy among CRN nodes. A visual representation Figure 11 illustrates the comparative performance of the proposed CH selection method using hybrid PSO and MFO optimization in terms of energy consumption. The x-axis represents the simulation time in seconds, while the y-axis depicts the energy consumption in joules for both the ECHRAC approach and the earlier baseline methods.

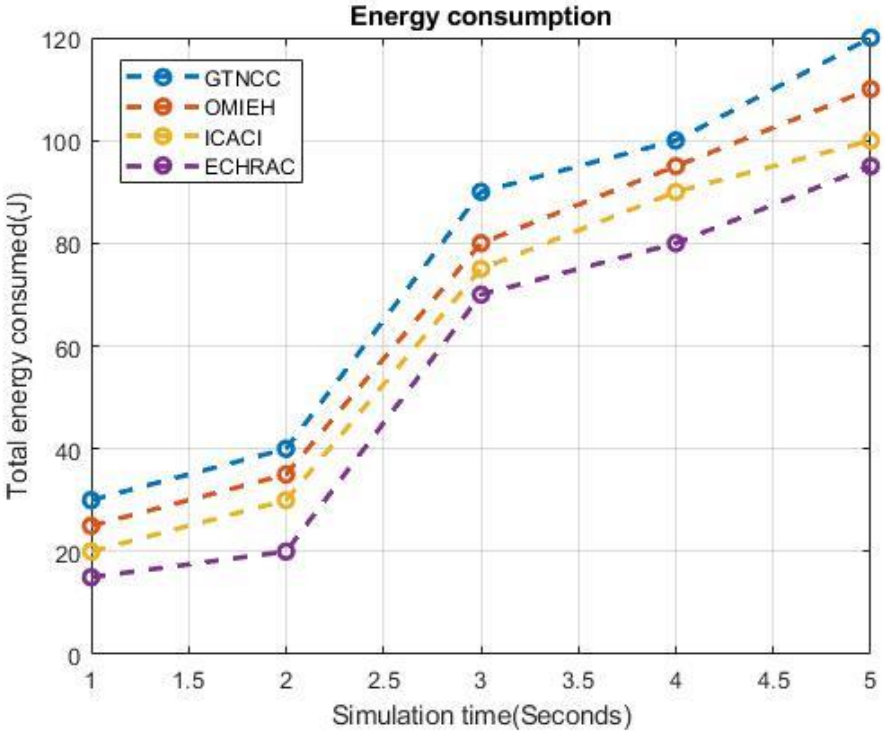

Figure 11 - Total Energy Consumption

Total Lifetime Calculation: In a network consisting of cluster-based hybrid PSO and MFO, the term "Total Lifetime" typically denotes the total operational duration or lifespan of the network, taking into account energy consumption and other relevant resources. The primary objective of the proposed ECHRAC, utilizing a hybrid PSO and MFO approach is to maximize the network's overall lifetime. Figure 12 visually illustrates the effective performance of CH selection and hybrid PSO-MFO optimization in the proposed ECHRAC, compared to previous baseline methods, in terms of total lifetime. On the horizontal axis, we have the simulation time measured in seconds, while the vertical axis shows the lifetime in seconds.

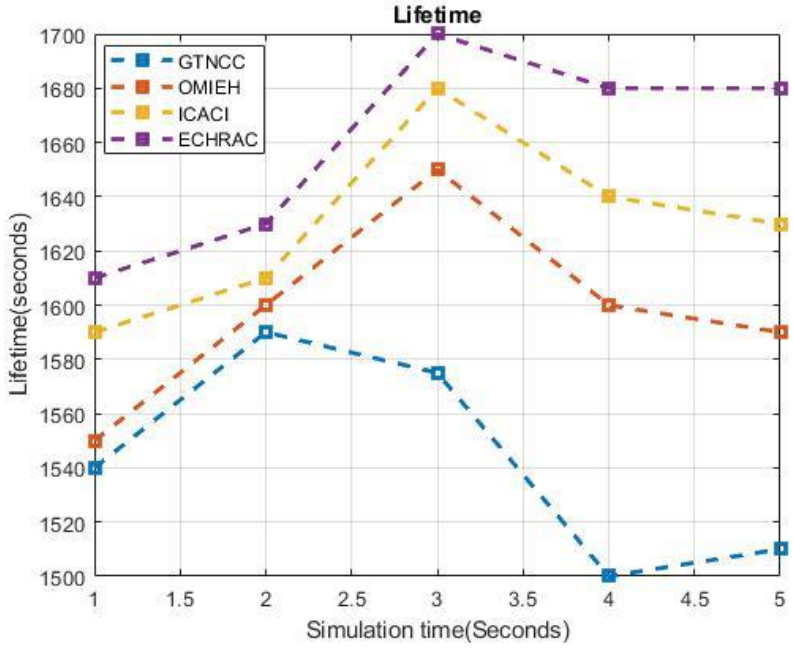

Figure 12 - Total Lifetime Calculation

Average Delay Calculation: "An efficient CH selection using a hybrid optimization-based CRN network involves calculating the average delay experienced by data packets as they travel through the network. This delay, measured in seconds, is a crucial performance indicator in CRN networks and reflects the time it takes for data packets to reach their destination from the source. A visual representation of this performance, as shown in Figure 13, compares the proposed ECHRAC method's use of CH selection and hybrid optimization to previous baseline methods, displaying the occurrence of average delay during data transmission between CRN nodes over simulation time on the x-axis and delay time on the y-axis."

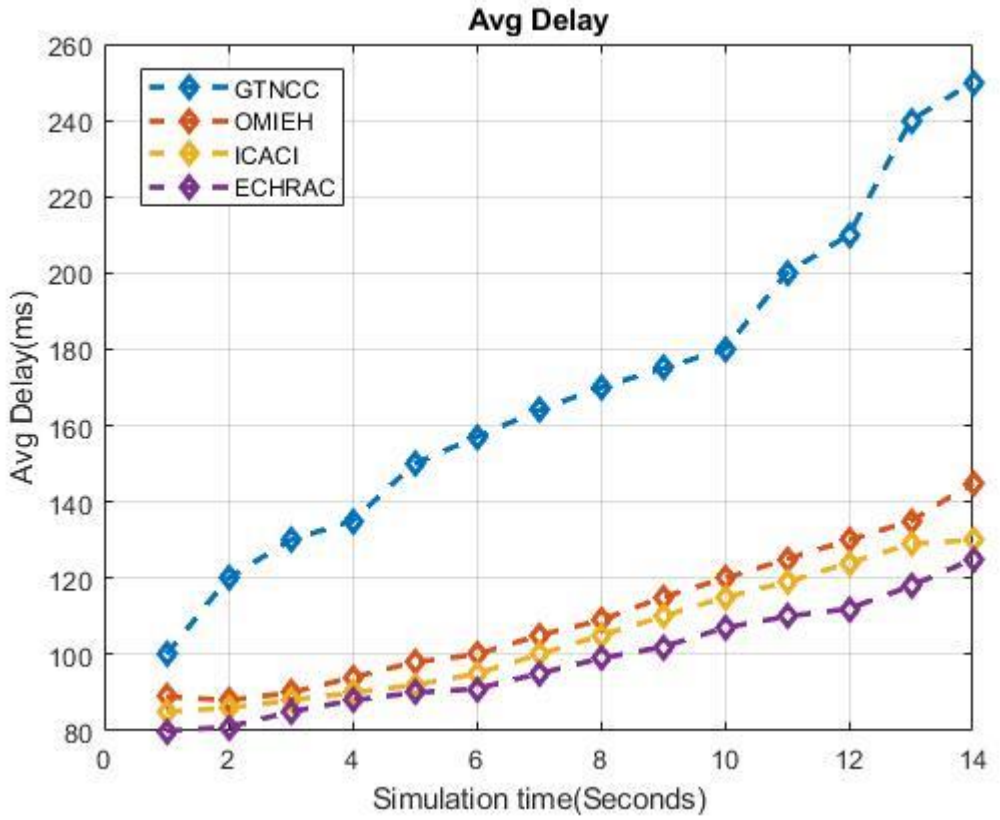

Figure 13 - Average Delay Calculation

Average Detection Rate: In a CRN that operates on a cluster-based system, the term "Average Detection Rate" typically describes the mean speed at which the network can recognize and classify PUs or signals within the available spectrum. The detection rate is an important measure in CRNs as it reflects how effectively the network can detect and respond to PUs or significant events. Figure 14 illustrates how the ECHRAC method, which utilizes CH selection and hybrid optimization, compares to previous methods by displaying the average detection rate during data transmission the x-axis represents the count of CRN nodes, while the y-axis indicates the amount of SUs.

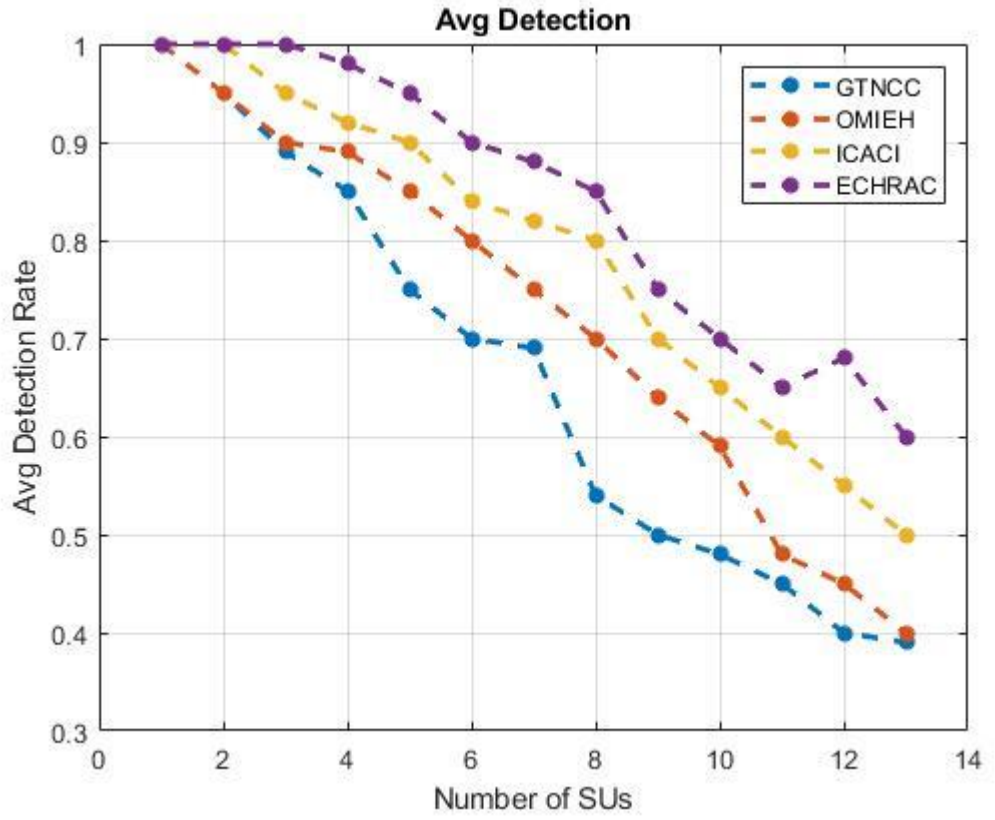

Figure 14 - Average Detection Rate

Average Throughput: The rate of successful data transmission in CRNs is known as throughput, which can be enhanced by combining CH selection and hybrid optimization. This metric is crucial in evaluating the effectiveness of data transfer and communication within the CRN and is usually measured in bps or a similar unit. To illustrate the impact of the ECHRAC method, which utilizes both CH selection and hybrid optimization, on throughput, Figure 15 shows a comparison with previous methods by plotting on the horizontal axis, we have the simulation time, and on the vertical axis, we observe the corresponding throughput rate calculations.

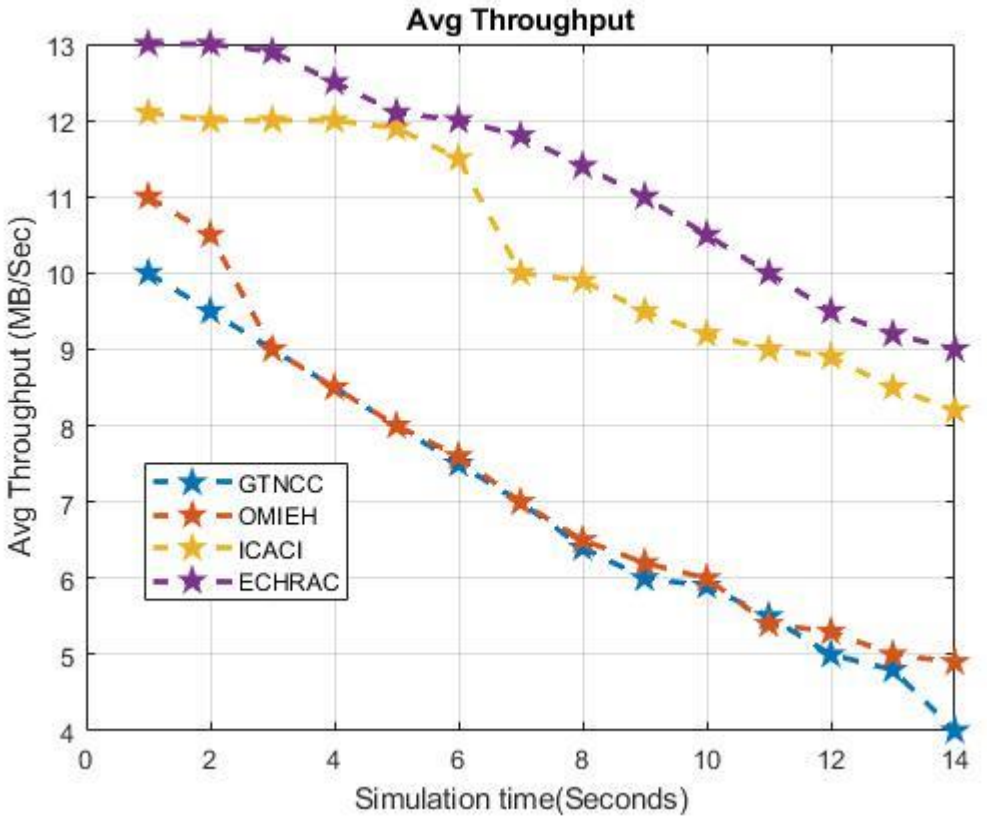

Figure 15 - Average Throughput

The ECHRAC model, which combines PSO and MFO, exhibits significant improvements in CRNs through the optimization of CH selection and allocation. ECHRAC is shown to reduce overall energy consumption by distributing more energy efficiently amongst the cluster's CRN nodes. A longer lifespan is achieved by this, enabling nodes to operate for extended periods. By using ECHRAC, the average delay data packets experience during transmission is greatly reduced, which is a critical factor in maintaining network responsiveness in CRNs. PUs is detected at a high rate in the model, which facilitates their classification within the spectrum with greater accuracy and faster detection time. It is especially critical when dealing with adaptive CRNs, which are slow to be detected and do not cause interference. By achieving a higher success rate in data transmission, the ECHRAC model surpasses traditional methods of measuring throughput, which is crucial for evaluating network efficiency. ECHRAC's convergence plot indicates that the hybrid PSO-MFO optimization rapidly converges into optimal solutions. The algorithm is proven to be effective in identifying stable configurations for CH without being restricted to local minima. The model's error rates are consistently low for different threshold values, as demonstrated by the error rate analysis. ECHRAC's optimization process is demonstrated by this, indicating its compatibility with the network requests. Well-formed cluster structures are produced by the model's assignment of clusters and centroid measurements, which balance the load among CHs while facilitating efficient intra-cluster communication. ECHRAC can achieve a balance between energy efficiency, communication delay, detection accuracy, and data throughput by using these metrics. The solution is both robust and effective for dynamic CRNs that require resource allocation. Overall, the research indicates that ECHRAC improves individual performance measures and leads to a holistic approach to CRN resource management. It also highlights the model's potential as a flexible and scalable model for energy-constrained, high-performance networks.

Conclusion

In conclusion, the integration of Enhanced CH Selection with Hybrid PSO and Modified MFO in CRNs represents a significant advancement in optimizing resource allocation and cluster management among the CR nodes. The hybrid nature of the proposed ECHRAC approach leverages the strengths of both PSO and Modified MFO to address the challenges associated with dynamic spectrum access and utilization of resources in CR nodes. Extensive simulations have validated the effectiveness of the

algorithm, considering various scenarios and network setups. The parameters involved in the comparative analysis include total energy consumption, network lifetime, average throughput, average delay, and average detection rate. The results of the comparative analysis demonstrate that the proposed ECHRAC approach outperformed earlier baseline methods, particularly in terms of network lifetime and throughput. This achievement signifies the potential for high-quality communication in CRNs using this approach. While the proposed ECHRAC approach exhibits promising results, ongoing research, and development could explore additional enhancements and extensions. Future work might focus on incorporating machine learning techniques, considering security aspects, or addressing specific challenges related to emerging technologies in CRNs.

References

[1] Wali Ullah Khan, Guftaar Ahmad Sardar Sidhu, et.al, “Fair power allocation in cooperative cognitive systems under NOMA transmission for future IoT networks”, Alexandria Engineering Journal, vol. 61, pp. 575–583, 2022, doi: 10.1016/j.aej.2021.04.107

[2] Tangwen Xu, Zhenshuang Li, et.al, “A Survey on Spectrum Sharing in Cognitive Radio Networks”, KSII Transactions on Internet and Information Systems, Egyptian Informatics Journal, vol. 21, pp. 231–239, 2020, doi: 10.1016/j.eij.2020.02.003

[3] Mohammed Saeed Alkatheiri, Ahmedin Mohammed Ahmed, et.al, “AODV routing protocol for Cognitive radio access based Internet of Things (IoT)”, Future Generation Computer Systems, no. 17, pp. 31920-92018, 2017, doi: 10.1016/j.future.2017.12.060

[4] Haythem Bany Salameh, Safa Otoum, et.al, “Intelligent Jamming-aware Routing in Multi-hop IoT-based Opportunistic Cognitive Radio Networks”, Ad Hoc Networks, no. 19, pp. 30636-5, 2020, doi: 10.1016/j.adhoc.2019.102035

[5] Ahmed H. Khalifa, Mohamed K. Shehata, et.al, “Enhanced cooperative behavior and fair spectrum allocation for intelligent IoT devices in cognitive radio networks”,Physical Communication, vol. 43, pp. 101190, 2020, doi: 10.1016/j.phycom.2020.101190

[6] Vimal Shanmuganathan, Manju Khari, et.al, “Energy Enhancement using Multi-objective Ant Colony Optimisation with Double Q-Learning Algorithm for IOT Based Cognitive Radio Networks”, Computer Communications, vol. 154, pp. 481–490, 2020 , doi: 10.1016/j.comcom.2020.03.004

[7] Ramsha Ahmed, Yueyun Chen, et.al, “CR-IoTNet: Machine learning based joint spectrum sensing and allocation for cognitive radio enabled IoT cellular networks”, Ad Hoc Networks, no. 20, pp. 30725-3, 2021, doi: 10.1016/j.adhoc.2020.102390

[8] Ismaeel Al Ridhawi, Khalaf Bataihah, et.al, “A multi-stage resource-constrained spectrum access mechanism for cognitive radio IoT networks: Time-spectrum block utilization”, Future Generation Computer Systems, no. 19, pp. 32486-0, 2020, doi: 10.1016/j.future.2020.04.022

[9] Sebastian Böhm, Michael Kirsche, “Radio-in-the-Loop Simulation and Emulation Modeling for Energy-Efficient and Cognitive Internet of Things in Smart Cities: A Cross-Layer Optimization Case Study”, Computer Communications, no. 24, pp. 00046-X, 2024, doi: 10.1016/j.comcom.2024.02.006.

[10] Ashutosh Sharma, Alexey Tselykh, et.al, “Throughput optimization of interference limited cognitive radio-based Internet of Things (CR-IoT) network”, Journal of King Saud University - Computer and Information Sciences, vol.34, pp. 4233–4243, 2022, doi: 10.1016/j.jksuci.2022.05.019

[11] Maliha Amjad, Ashfaq Ahmed, et.al, “Resource Management in Energy Harvesting Cooperative IoT Network under QoS Constraints”, Digital Communications and Networks, no. 23, pp. 00019-6, 2023, doi: 10.1016/j.dcan.2023.01.006

[12] Muhammad Arif Mughal, Ata Ullah, et.al, “An intelligent channel assignment algorithm for cognitive radio networks using a tree-centric approach in IoT”, Alexandria Engineering Journal, vol. 91, pp. 152–160, 2024, doi: 10.1016/j.aej.2024.01.071

[13] Zhen Li, Tao Jing, et.al, “Worst-Case Cooperative Jamming for Secure Communications in CIoT Networks”, Sensors, vol. 16, pp. 339, 2016, doi: 10.3390/s16030339

[14] Xiong Luo, Zhijie He, et.al, “Resource Allocation in the Cognitive Radio Network-Aided Internet of Things for the Cyber-Physical-Social System: An Efficient Jaya Algorithm”, Sensors, vol. 18, pp. 3649, 2018, doi: 10.3390/s18113649

[15] Muhammad Shafiq, Maqbool Ahmad, et.al, “Handshake Sense Multiple Access Control for Cognitive Radio-Based IoT Networks”, Sensors, vol. 19, pp. 241, 2019, doi: 10.3390/s19020241

[16] Jun Wang, Weibin Jiang, et.al, “Multiband Spectrum Sensing and Power Allocation for aCognitive Radio-Enabled Smart Grid”, Sensors, vol. 21, pp. 8384, 2021, doi: 10.3390/s21248384

[17] Dr Shahzad Latif, et.al, “An Efficient Pareto Optimal Resource Allocation Scheme in Cognitive Radio-Based Internet of Things Networks”, Sensors, v0l . 22, pp. 451, 2022, doi: 10.3390/s22020451

[18] Xavier Fernando, George Lăzăroiu, “Spectrum Sensing, Clustering Algorithms, and Energy-Harvesting Technology for Cognitive-Radio-Based Internet-of-Things Networks”, Sensors, vol. 23, pp. 7792, 2023, doi: 10.3390/s23187792

[19] Osamah Ibrahim Khalaf, Kingsley A. Ogudo, et.al, “A Fuzzy-Based Optimization Technique for the Energy and Spectrum Efficiencies Trade-Off in Cognitive Radio-Enabled 5G Network”, Symmetry, vol. 13, pp. 47, 2020, doi: 10.3390/sym13010047

[20] Stalin Allwin Devaraj, Kambatty Bojan Gurumoorthy, et.al, “Cluster-ID-Based Throughput Improvement in Cognitive Radio Networks for 5G and Beyond-5G IoT Applications”, Micromachines, vol. 13, pp. 1414, 2022, doi: 10.3390/mi13091414

[21] Shalley Bakshi, Surbhi Sharma, et.al, “Shapley-Value-Based Hybrid Metaheuristic Multi-Objective Optimization for Energy Efficiency in an Energy-Harvesting Cognitive Radio Network”, Mathematics, vol. 11, pp. 1656,2023, doi: 10.3390/math11071656

[22] Adamantia Stamou, Grigorios Kakkavas, et.al, “Autonomic Network Management and Cross-Layer Optimization in Software Defined Radio Environments”, Future Internet, vol. 11, pp. 37, 2019, doi: 10.3390/fi11020037

[23] Shuang Fu, Dailin Jiang, “Multi-Dimensional Resource Allocation for throughput Maximization in CRIoT with SWIPT”, Energies, vol. 16, pp. 4767, 2023, doi: 10.3390/en16124767

[24] Tian Yang, Moez Esseghir, et.al, “Evaluation of Primary User Power Impact for Joint Optimization of Energy Efficiency in Cognitive Radio Networks”, Energies, vol. 14, pp. 701, 2021, doi: 10.3390/en14217012

[25] Ayman A. El-Saleh, Tareq M. Shami, et.al, “Multi-Objective Optimization of Joint Power and Admission Control in Cognitive Radio Networks Using Enhanced Swarm Intelligence”, Electronics, vol. 10, pp. 189, 2021, doi: 10.3390/electronics10020189

[26] Prativa Rai, MK Ghose, et.al, “Game theory based node clustering for cognitive radio wireless sensor networks”, Egyptian Informatics Journal, vol. 23, pp. 315–327, 2022, doi: 10.1016/j.eij.2022.02.003

[27] Van-Truong Truong, Dac-Binh Ha, et.al, “Performance analysis and optimization of multiple IIoT devices radio frequency energy harvesting NOMA mobile edge computing networks”, Alexandria Engineering Journal, vol. 79, pp. 1–20, 2023, doi: 10.1016/j.aej.2023.07.025

[28] Muhammad Arif Mughal, Ata Ullah, et.al, “An intelligent channel assignment algorithm for cognitive radio networks using a tree-centric approach in IoT”, Alexandria Engineering Journal, vol. 91, pp. 152–160, 2024, doi: 10.1016/j.aej.2024.01.071.